

LCLC Converter With Optimal Capacitor Utilization for Hold-Up Mode Operation

Yang Chen ^{ID}, Member, IEEE, Hongliang Wang ^{ID}, Senior Member, IEEE, Zhiyuan Hu ^{ID}, Member, IEEE, Yan-Fei Liu ^{ID}, Fellow, IEEE, Xiaodong Liu, Jahangir Afsharian, and Zhihua Yang

Abstract—In data center and telecommunication power supplies, the front-end dc–dc stage is required to operate with a wide input voltage range to provide hold-up time when ac input fails. Conventional LLC converter serving as the dc–dc stage is not suitable for this requirement, as the normal operation efficiency (at 400 V input) will be penalized once the converter is designed to achieve high peak gain (wide input voltage range). This paper examined the operation of the LCLC converter and revealed that the LCLC converter could be essentially equivalent to a set of LLC converters with different magnetizing inductors that are automatically adjusted for different input voltages. In nominal 400 V input operation, the LCLC converter behaves like an LLC converter with large magnetizing inductor, thus the resonant current is small. In the hold-up period, when the input voltage reduces, the equivalent magnetizing inductor will reduce together with switching frequency reducing, thus the converter achieves high peak gain. In this paper, a new design methodology is also proposed to achieve optimal utilization of the two resonant capacitors for high power application. To verify the effectiveness of the LCLC converter for hold-up operation, comprehensive analysis has been conducted; a detailed step by step design example based on capacitor voltage stress is introduced; an experimental LCLC prototype optimized at 400 V, with input voltage range of 250–400 V and 12 V/500 W as output has been presented.

Index Terms—High voltage gain, hold up, LLC, multielement resonant, wide input voltage range.

I. INTRODUCTION

THE RAPID growth of power consumption in server and data center power systems has been driving the performance improvement of the power supply in recent years [1], [2]. In a server power supply, the front-end converter connects

Manuscript received July 2, 2017; revised October 24, 2017 and February 13, 2018; accepted May 17, 2018. Date of publication May 29, 2018; date of current version February 5, 2019. This work was supported by the Natural Sciences and Engineering Research Council of Canada (NSERC). Recommended for publication by Associate Editor T. Qiang. (Corresponding author: Hongliang Wang.)

Y. Chen and Y.-F. Liu are with the Department of Electrical and Computer Engineering, Queen's University, Kingston, ON K7L 3N6, Canada (e-mail: yang.chen@queensu.ca; yanfei.liu@queensu.ca).

H. Wang is with the College of Electrical and Information Engineering, Hunan University, Changsha 410082, China (e-mail: liangliang-930@163.com).

Z. Hu is with the Apple Inc., Cupertino, CA 95014 USA (e-mail: zhiyuan.hu@queensu.ca).

X. Liu is with the School of Electrical Engineering and Information, Anhui University of Technology, Maanshan 243000, China (e-mail: liuxiaodong@ahut.edu.cn).

J. Afsharian and Z. Yang are with the Murata Power Solutions, Toronto, ON L3R 0J3, Canada (e-mail: jafsharian@murata.com; ZYang@murata.com).

Color versions of one or more of the figures in this paper are available online at <http://ieeexplore.ieee.org>.

Digital Object Identifier 10.1109/TPEL.2018.2842022

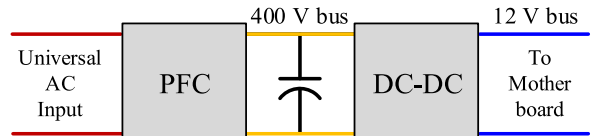


Fig. 1. Structure of the front-end converter.

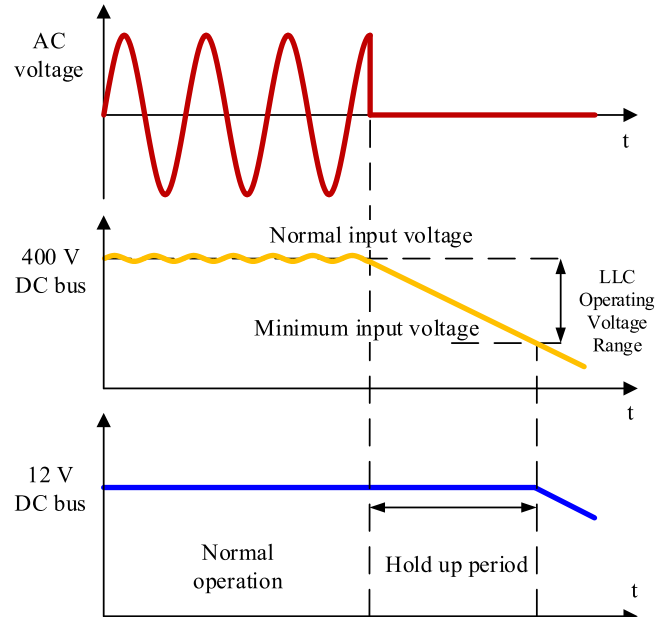


Fig. 2. Hold-up problem process.

the ac grid and outputs 12 V dc (or emerging 48 V). The 12 V dc bus is then connected to the motherboard inside the server to power the point of load converter for CPUs and other parts. Fig. 1 shows the typical structure of the front-end ac to dc converter in the data center power system. A power factor correction stage rectifies the ac line into 400 V dc, which is further converted by a dc–dc stage into 12 V [3]–[5].

A critical issue for data center power supply is the hold-up problem illustrated in Fig. 2. When the ac line fails, the 400 V bus voltage reduces continuously as the energy storage capacitor discharges. The dc–dc stage converter is then required to operate with a bus voltage that is lower than the designed level (i.e., 400 V), so that a period of time can be saved for the UPS to react. In this way, the load or the end converters will not “feel” the interrupt on the ac side. Usually, the hold-up period

lasts for several tens of milliseconds [5]. If the operation range of the dc–dc converter is extended, the capacitor value used on the 400 V bus can be reduced, then the cost will drop and size will reduce significantly. Therefore, improving the operational input voltage range, i.e., the voltage gain of the dc–dc converter, is the solution to the hold-up issue.

LLC resonant converter is widely used as the dc–dc stage due to its high efficiency as a result of the inherent zero voltage switching (ZVS) for the primary MOSFETs and zero current switching (ZCS) for the secondary rectifiers [3]–[7]. However, designing the *LLC* converter with hold-up ability could compromise its high performance in normal operation. It is widely acknowledged that if the *LLC* converter is designed to achieve high voltage gain, a small magnetizing inductor value should be used. Such design could lead to severe conduction loss in the primary side for normal operation at 400 V input [8], [9]. Therefore, to solve the hold-up problem, the *LLC* converter should be improved to meet the following requirements:

- 1) to achieve high efficiency for the nominal 400 V input operation;
- 2) to increase the operational input voltage range.

To achieve high efficiency at 400 V operation, from the point of view of parameter design, the transformer turns-ratio needs to be properly designed to ensure that the converter operates at resonant frequency for 400 V input. Besides, the magnetizing inductor value should be optimized to reduce the current stress in the resonant tank as much as possible while maintaining ZVS for the half-bridge (HB) MOSFETs. At last, for 12 V output applications, on the secondary side, synchronous rectifiers (SRs) should be used instead of diode rectifiers, as the forward voltage drop of diodes would be a deal breaker of the whole efficiency [10]–[12].

To meet the hold-up time requirement, quite a few methods have been proposed. Before the age of *LLC* converters, a baby boost converter is used for asymmetrical HB converters to achieve hold-up operation [13]. Similarly, a baby boost converter can reduce the burden of the *LLC* stage, although *LLC* converters are step-up converters with hold-up ability by its own nature. However, the additional power stage will reduce the efficiency at nominal 400 V operation. Besides, the two stage configuration is complicated, and, consequently, costly.

Another method solves the hold-up problem by utilizing auxiliary windings on the secondary side of the main transformer for both PWM converter [14], and *LLC* converters [15]. Generally speaking, as long as the input voltage reduces below the designed range, the switch-controlled auxiliary windings will take over the secondary side power transfer. Increased transformer turns-ratio helps achieve higher output-to-input voltage gain during the hold-up period. The independent circuit designs between nominal 400 V operation and hold-up mode operation can maintain 400 V input operation uninfluenced. However, usually the main transformer is the most bulky and lossy part of a converter, thus adding extra windings makes it even more difficult to optimize the transformer from both efficiency and power density improvement point of view.

By driving the HB MOSFETs with asymmetric pulse width modulation (APWM) rather than conventional frequency modulation (FM), *LLC* converter can improve voltage gain without

any additional components [16]. This method, however, suffers from limited peak gain enhancement. Besides, once the resonant tank is designed, the maximum gain that APWM control could achieve is also determined. Thus, in order to satisfy the voltage gain requirement, the resonant parameters design might not be optimized for 400 V operation.

A critical insight was revealed in [17] that if the resonant tank can be charged with more energy during one switching cycle, *LLC* converter achieves higher gain. To charge the resonant tank more, the secondary windings are short circuit for a certain period of time in every switching cycle. The downside of this method is that quite a few components need to be added in the power train on the secondary side, which causes size increasing and efficiency reducing.

Based on [17], a few improving methods propose to adopt either boost PWM discontinuous current mode (DCM) control [18] or phase shift control on *LLC* topology [19], [20]. The common principle of these methods is that, in each switching cycle, the resonant tank will be short circuit on either primary side or secondary side by auxiliary switches for a period of time, so that the resonant inductor can be energized more quickly, hence store and transfer more power. The nominal 400 V efficiency remains uninfluenced as compared to a conventional *LLC* optimized for 400 V input voltage. However, during the hold-up period, the converter is operating at DCM, thus both primary and secondary components have significantly higher current stress as compared to 400 V operation, which potentially calls for overdesign in terms of component selection. Besides, these methods use full-bridge rectifier with diodes, thus are not suitable in low output voltage applications.

In [21] and [22], Wang *et al.* have proposed *LLC* converter with auxiliary switch on the primary side to reduce the current stresses, and solves the SR problem. The potential drawback is that the auxiliary switch achieves no soft switching, which limits the maximum switching frequency.

Four-element resonant topologies have been studied and reported to achieve better performance than *LLC* converter in various aspects, e.g., the startup process, current limiting ability, and load regulation. In this paper, *LCLC* resonant topologies will be revisited from increasing the voltage gain point of view [23]. In 400 V normal operation, the *LCLC* converter is equivalent to an *LLC* converter with a large magnetizing inductor, so that the magnetizing current that is circulating on the primary side will be low, and 400 V efficiency is high. For hold-up operation, when the input voltage reduces, the magnetizing inductor reduces along with the switching frequency, thus the output-to-input voltage gain increases, and the operational input voltage range is extended. Unlike the aforementioned *LLC* converter with PWM control, *LCLC* converter can be implemented with existing controller that is designed for conventional *LLC* converter, which reduces the overall developing time and cost. Besides, *LCLC* converter works with SR, thus it is beneficial for low output voltage applications. Moreover, *LCLC* converter utilizes pure passive components, avoiding cumbersome sensing and sudden operation changes, thus it is specifically suitable for high power applications which require high reliability.

This paper is organized as follows: Section II describes the operation principle of the *LCLC* converter from dc voltage gain point of view; Section III discusses a design methodology based on capacitor voltage stresses; Section IV demonstrates the experimental results; and Section V concludes the paper.

II. PRINCIPLE ANALYSIS OF *LCLC* CONVERTER FROM DC GAIN POINT OF VIEW

The discussion in this section can be separated in three parts: part A will discuss the desired performance of the *LLC* converter in hold-up applications; part B will discuss the operation of the *LCLC* converter, and prove that the *LCLC* converter meet the desired performance; part C will discuss the differences in magnetics component design as compared to the *LLC* converter.

A. Desired Performance for Hold-Up Operation and *LLC* Limitation

In data center applications, high voltage gain is required to satisfy the wide input voltage range and/or hold-up requirements. The limitation of conventional *LLC* converter is that it can only be optimized for one specific input voltage level or a narrow input voltage range near the resonant point. In the optimized parameters for normal 400 V operation, magnetizing inductor value is usually large, so the losses in the primary-side switches and the magnetic components are low. On the other hand, to achieve high voltage gain, the magnetizing inductor value should be small. Then, enough current can be generated to compensate the voltage difference between the source and sink of the resonant tank. This is the well-known contradiction between high voltage gain and high efficiency performances in terms of parameter design for *LLC* converter.

The limitation described above also implies the desired characteristic of *LLC* converter in the hold-up application—a magnetizing inductor L_m that changes for different input voltages. Specifically, for normal input at 400 V, the L_m should be of high value; and for low input voltages, the L_m should be of low value.

According to FM, the switching frequency is changing along with the input voltage in the same direction. Then, the desired characteristic of the magnetizing inductor could be interpreted as changing together with the switching frequency in the same direction. In other words, the large L_m at high switching frequency, and vice versa.

Fig. 3 shows the desired *LLC* performance for hold-up operation with different L_m and fixed L_r and C_r . The L_r of 16.5 μ H and C_r of 23.5 nF are from Table II for illustration purposes. When the input voltage is at 400 V, the switching frequency is at resonant point of 250 kHz, and the magnetizing inductor is high at 180 μ H. As the input voltage reduces to 250 V, the switching frequency reduces to 130 kHz. Then, the magnetizing inductor also reduces (to 70 μ H in this case), so the voltage gain is increased from 1.1 to 1.6, which in turn accommodates the reduced input voltage.

This desired autochanging magnetizing inductor L_m can be implemented by a pair of series-connected inductor L_p and capacitor C_p on the parallel branch of the resonant tank. From the

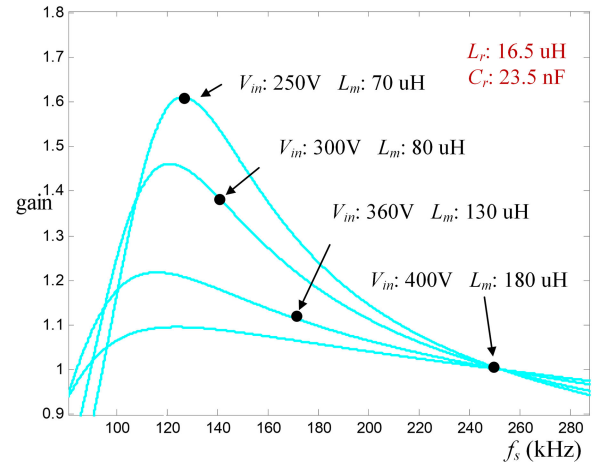


Fig. 3. Desired *LLC* with different L_m for hold-up operation ($L_r = 16.5 \mu$ H, $C_r = 23.5$ nF).

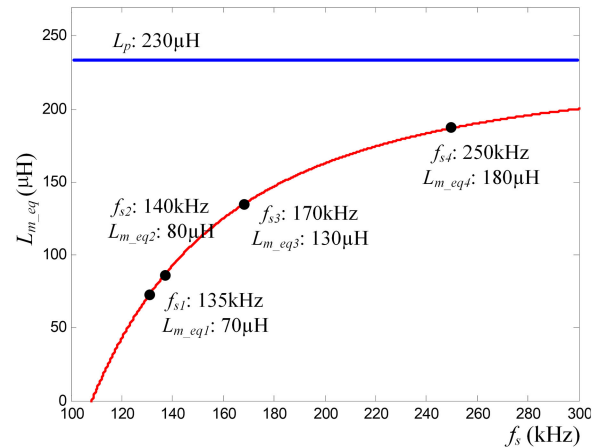


Fig. 4. Equivalent L_{m_eq} changing with f_s ($L_p = 230 \mu$ H, $C_p = 9.4$ nF).

point of view of impedance, a capacitor behaves like a negative inductor whose value changes with frequency in a reverse quadratic manner. For given L_p and C_p values, the equivalent magnetizing inductor L_{m_eq} at different switching frequency can be calculated by the following equation:

$$L_{m_eq}(f_s) = L_p - \frac{1}{(2\pi f_s)^2 C_p}. \quad (1)$$

From (1), it could be concluded that the performance of the L_{m_eq} is exactly as the desired—large at high frequency and small at low frequency, as long as the total impedance of L_p and C_p remains as inductive. Fig. 4 shows the L_{m_eq} value changing with switching frequency with L_p of 230 μ H and C_p of 9.4 nF (from Table II).

B. *LCLC* Converter Operation Principle

The *LCLC* converter topology is shown in Fig. 5, in which L_r and C_r are the series resonant inductor and capacitor, and L_p and C_p are parallel inductor and capacitor. V_{in} is the input dc voltage, V_o is the output dc voltage, and n is the transformer turns ratio.

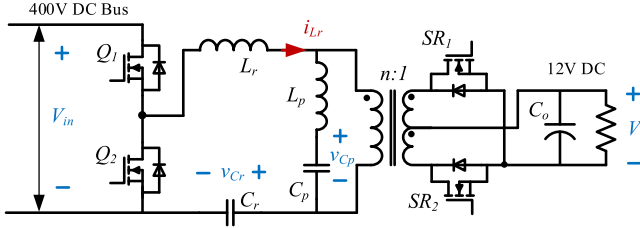


Fig. 5. *LCLC* converter topology with center tapped transformer and SR.

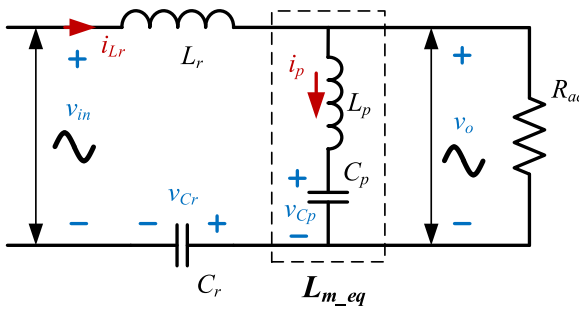


Fig. 6. First harmonic approximation of *LCLC* converter.

As compared with the *LLC* converter, C_p is added on the parallel branch. The value of C_p should be selected in such a way that the resonant frequency of L_p and C_p is lower than the entire switching frequency range. Then the impedance of L_p and C_p branch will always be inductive, and the *LCLC* converter can always be equivalent to *LLC* converters at different switching frequencies (input voltages). For normal 400 V operation at high switching frequency near the resonant point, the equivalent L_m is large, and high efficiency could be achieved. With switching frequency reducing, the equivalent L_m will reduce. As a result, the *LCLC* converter achieves higher gain when the input voltage is low.

The conventional first harmonic approximation (FHA) method is still valid for analyzing the *LCLC* converter and calculate the voltage gain. Fig. 6 shows the FHA model, in which v_{in} is the fundamental component of the input square-wave ac voltage seen by the resonant tank, and the RMS value of v_{in} equals to $\frac{2\sqrt{2}}{\pi} V_{in}$. v_o is the reflected ac output voltage, and the RMS value of v_o is $\frac{2\sqrt{2}}{\pi} n V_o$. R_{ac} is the equivalent load resistor in the resonant tank, and there is $R_{ac} = \frac{8n^2}{\pi^2} \cdot \frac{V_o^2}{P_o}$.

By the analyzing the FHA circuit of the *LCLC* converter in frequency domain, the voltage gain can be then calculated with $G = v_{in}/v_o$. Alternatively, the voltage gain can be calculated with the conventional *LLC* voltage gain equation as shown in (2) by replacing the variable L_m with the equivalent L_{m_eq} that is calculated by (1) at different switching frequencies. In (2), Q is the quality factor defined as $Q = \sqrt{L_r/C_r}/R_{ac}$

$$G = \frac{1}{\sqrt{\left(1 + \frac{L_r}{L_{m_eq}} - \frac{L_r}{L_{m_eq}} \left(\frac{f_r}{f_s}\right)^2\right)^2 + \left(Q \left(\frac{f_s}{f_r} - \frac{f_r}{f_s}\right)\right)^2}}. \quad (2)$$

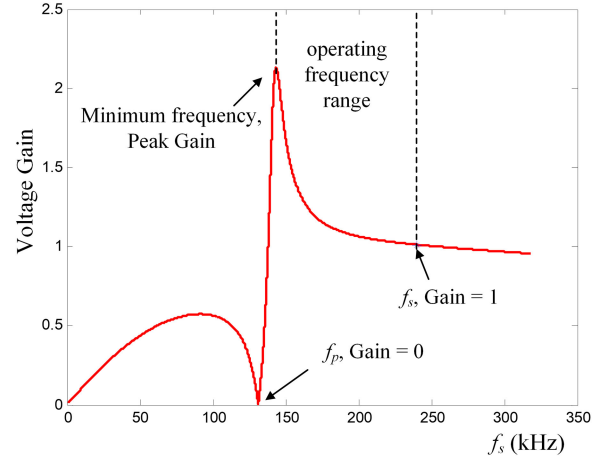


Fig. 7. Typical gain curve of *LCLC* converter.

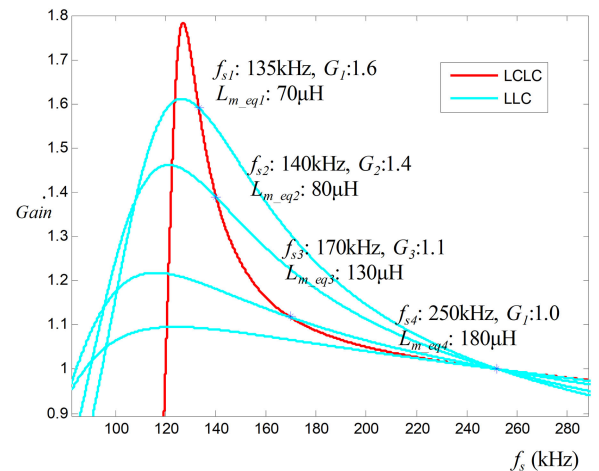


Fig. 8. *LCLC* gain curve fits the *LLC* gain curves at specific operating points ($L_r = 16.5 \mu\text{H}$, $C_r = 23.5 \text{ nF}$, $L_p = 230 \mu\text{H}$, $C_p = 9.4 \text{ nF}$).

Fig. 7 shows a typical gain curve versus switching frequency of the *LCLC* converter. Conventional FM can still be used. The parallel resonant frequency f_p of L_p and C_p should be designed lower than the series resonant frequency f_r , and the operation range should be limited between resonant point f_r and peak gain point f_{\min} , such that the voltage gain is monotonically changing with switching frequency, and ZVS for HB FETs and ZCS for SR FETs can be achieved. It should be noted that the voltage gain is zero at the parallel resonant frequency f_p , as the transformer primary side is short circuit.

Fig. 8 shows that the *LCLC* gain curve (in solid red) fits the desired gain curves (in light blue) of *LLC* converters with different L_m values. The parameters are from Table II.

At nominal of 400 V, the converter operates at the series resonant frequency 250 kHz. The corresponding gain is unity. The equivalent L_{m_eq} is 180 μH . As compared to the conventional *LLC* converter with L_m of 70 μH (for the same gain performance), this more than 2.5 times larger magnetizing inductor will significantly reduce the current in the resonant tank, so the conduction and switching loss in the MOSFETS as well as the

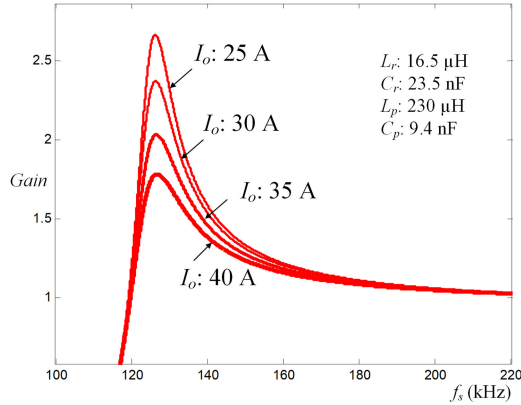


Fig. 9. LCLC gain curve at different load condition.

core loss and copper loss in the magnetic components would be significantly reduced.

The equivalent \$L_m\$ will reduce together with the switching frequency if the input voltage drops. At 135 kHz, the equivalent \$L_m\$ is \$70 \mu\text{H}\$. With this set of parameters, peak voltage gain is increased to more than 1.6 from 1.1 with \$L_m\$ of \$180 \mu\text{H}\$, so that the designed minimum input voltage could be as low as 250 V.

Fig. 9 shows the LCLC converter voltage gain changing with load current. As can be observed, the behavior is very similar to the conventional LLC converter. A noticeable difference is that while the LLC converter has lower peak gain frequency for lighter load, LCLC converters' peak gain frequencies converge to one point for different loads. This could be attributed to the parallel resonant frequency of \$L_p\$ and \$C_p\$. This characteristic will be beneficial for some applications that require the converter to operate as current source, i.e., always operate at the peak gain point.

In terms of operation modes, LCLC converter is same as LLC converters, because the LCLC converter can be equivalent to LLC converters over the entire operation range. In each switching cycle, the circuit behaviors during the switch conducting period and dead time are exactly same for LCLC converter and its equivalent LLC converters. Besides, the switching logic and the control are also the same. Thus, the existing controller for the LLC converter can be directly used.

Although the LCLC converter can be understood and designed from the equivalent LLC point of view, special attention should be paid to the parallel capacitor \$C_p\$. In Fig. 6, it is observed that the parallel branch of \$L_p\$ and \$C_p\$ has fixed voltage stress of \$v_o\$. As the total impedance is inductive (as \$L_{m,\text{eq}}\$), at given switching frequency, the parallel branch can be viewed as a current source, and the peak value \$i_{p,\text{pk}}\$ can be determined by (3), in which \$L_{m,\text{eq}}\$ is given by (1)

$$i_{p,\text{pk}} = \frac{v_o}{2\pi f_s L_{m,\text{eq}}} = \frac{4}{\pi} nV_o \frac{2\pi f_s C_p}{(2\pi f_s)^2 L_p C_p - 1}. \quad (3)$$

Then, the voltage stress on \$C_p\$ can be calculated by the following equation:

$$v_{Cp,\text{pk}} = i_{p,\text{pk}} \frac{1}{2\pi f_s C_p} = \frac{4}{\pi} nV_o \frac{1}{(2\pi f_s)^2 L_p C_p - 1}. \quad (4)$$

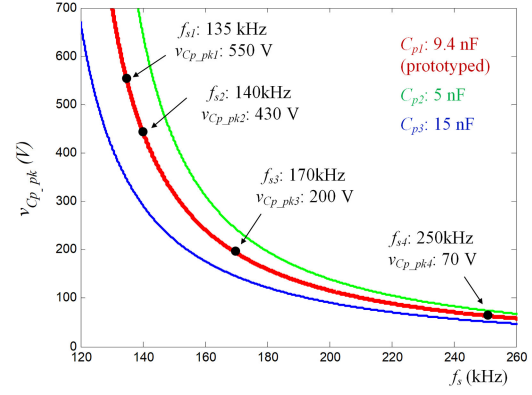


Fig. 10. Voltage stress on \$C_p\$ at different switching frequencies.

Fig. 10 shows the voltage stresses on different capacitor value of \$C_p\$ changing with switching frequency. At low input voltage region, i.e., low switching frequency, the voltage stress increases sharply, because both the current stress and the capacitor impedance increase with the switching frequency reducing, and their product grows in a reverse quadratic relationship. Thus, during the design, the peak voltage stress at minimum input voltage should be carefully designed.

In Fig. 10, the voltage stress of three capacitor values is also compared. The red line shows the calculated peak voltage stress for the parameter design in Table II. All three designs have same peak voltage gain, i.e., same \$L_{m,\text{eq}}\$ of \$70 \mu\text{H}\$ at minimum frequency of 135 kHz. It has been analyzed that larger \$L_p\$ is preferred to reduce circulation loss. To achieve so, smaller \$C_p\$ should be used. However, it is observed in Fig. 10 that smaller \$C_p\$ will have larger peak voltage stress, which could limit the choice and require tradeoff in practical designs. More details will be revealed in a Section III.

C. \$L_p\$ and \$C_p\$ Implementation and Magnetics Design Considerations

In conventional LLC converters, the \$L_p\$ is usually afforded by the magnetizing inductor \$L_m\$ of the transformer. Such design could reduce the size and weight of the total magnetic components to the minimum. In LCLC converter, the \$L_p\$ and \$C_p\$ should be external. As shown in the prototype picture in the Experiment section, the total space consumed by the external \$L_p\$ and \$C_p\$ is \$3.2 \text{ cm} * 3 \text{ cm} * 5 \text{ cm}\$, which is less than 10% of the total volume measuring as \$10 \text{ cm} * 10 \text{ cm} * 5 \text{ cm}\$. This size increase is believed affordable.

For LLC used in low power applications, e.g., below 500 W, magnetic integration is usually a preferred choice. However, if the power is higher, magnetic integration is not always desired. It is already an accepted practice in the industry to use separate cores when the efficiency performance becomes the primary target. The reason is that the conduction loss takes an overwhelming part, while the core loss is relatively minor in high current application. By employing an external \$L_p\$, the transformer primary current is separated for two conductors, thus the primary conduction loss will be reduced. In most cases, the conduction loss reduction will outnumber the additional core

loss of L_p . Thus, an external L_p is not necessarily unprofitable. Besides, since a separate L_p is used, the air gap on the transformer can be removed. This generates no additional core loss, but removes the fringing loss caused by the air gap.

Therefore, the *LCLC* converter trades for higher performance with affordable size compromise. With the external L_p , an ungapped transformer can be used in the *LCLC* converter, which is expected to be of smaller size and/or higher performance over the conventional *LLC* transformers. This advantage is even more competitive for planar transformers, which suffer from limited window size and generally heavier conduction loss.

III. *LCLC* CONVERTER DESIGN METHODOLOGY BASED ON CAPACITOR VOLTAGE STRESS

Extensive design methods have been proposed for *LLC* converter in different applications [24]–[30]. These optimal design methods place no limit on capacitor voltage stress, which in practice may bring about iterative capacitor calibrations, especially in high power applications. It has been observed that the ac voltage stress on the resonant capacitor can be as high as 1 kV in 500 W and above applications. High voltage stress on the capacitor not only increases the cost, but also reduces the reliability. Especially when C_p is added, it is essential to balance the voltage stresses on both capacitors to achieve optimal capacitor utilization. Based on this criterion, a design methodology based on the capacitor voltage stress is proposed in this paper. The design method considers primarily two equivalent *LLC* converters—equivalent *LLC* design for minimum input voltage (250 V) based on voltage gain requirement; and equivalent *LLC* design for normal operation (400 V) evaluated from the efficiency point of view. The design logic is described below and the design flow chart is shown in Fig. 11.

- 1) *Specification*: In this step, the input voltage range should be specified—including the maximum input voltage V_{in_max} , at which the converter normally operates, and minimum input voltage V_{in_min} during the hold-up process. The transformer turns-ratio n should be selected based on the V_{in_max} and the rated output voltage V_o , so that the converter will operate at the specified resonant frequency f_r for normal operation. The relationship can be determined by $n = V_{in_max}/(2V_o)$ for HB in this case.
- 2) *Equivalent LLC design for V_{in_min} (250 V)*: According to FM, the switching frequency for minimum input voltage V_{in_min} is the minimum frequency f_{min} , at which the converter will achieve the peak voltage gain. In this design procedure, the selection of f_{min} will require the designer's engineering judgement. Then, the value of minimum C_r , and corresponding L_r , and equivalent magnetizing inductor L_{m_min} for V_{in_min} could be determined based on the C_r voltage stress.
- 3) *Equivalent LLC design for V_{in_max} (400 V)*: The L_r value and C_r value should remain the same as that in the last step. Equivalent L_m should be increased for V_{in_max} so as to reduce the current stress in the resonant tank. The maximum equivalent L_{m_max} is limited by the C_p voltage stress.

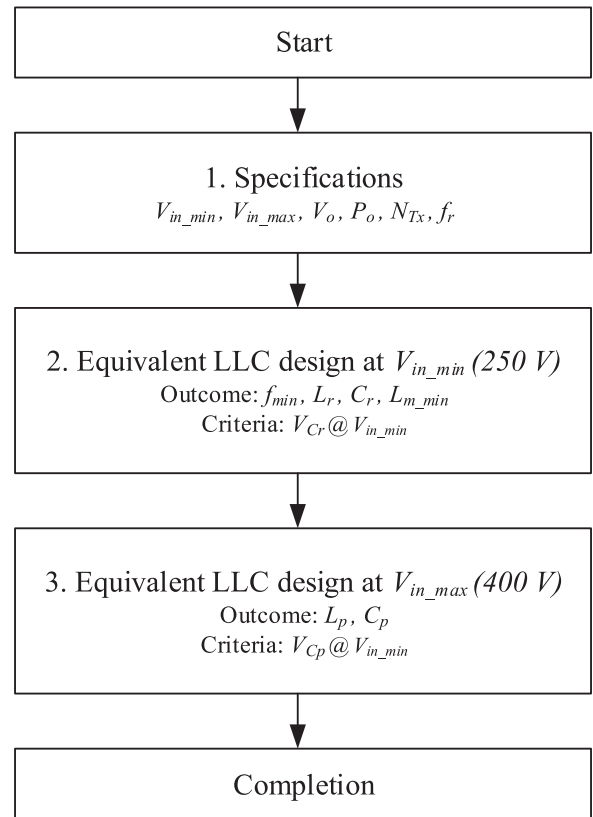


Fig. 11. Design flowchart of the proposed design method based on capacitor voltage stress.

To help demonstrate the design methodology, a detailed design example is given in the following part.

A. Specification

The design is based on a 250–400 V input, 12 V/500 W output application. Theoretically, the turns-ratio of the transformer should be 16.7:1 ($n = V_{in_max}/(2V_o) = 400 \text{ V}/(2 * 12\text{V})$) to ensure that the normal operation at 400 V is at the resonant point. In real world, the turns-ratio is chosen as 17:1, so that the voltage gain is slightly above unity, and the secondary rectifiers will have ZCS operation.

The series resonant frequency f_r should be chosen based on the designer's engineering judgement to optimize the efficiency at 400 V normal operation. The consideration of f_r selection should include but not limited to the magnetic components design and fabrication, thermal design, and tradeoff of the conduction loss and switching loss in the switching device, and so on. In this design example, the series resonant frequency is chosen at 250 kHz according to the experience by the authors concerning the above-mentioned aspects.

B. Selection of Minimum Switching Frequency for 250 V

LCLC converter follows the same FM as conventional *LLC* converter, i.e., switching frequency reduces along with input voltage reducing. Thus, the switching frequency at 250 V operation should be the minimum switching frequency f_{min} for the

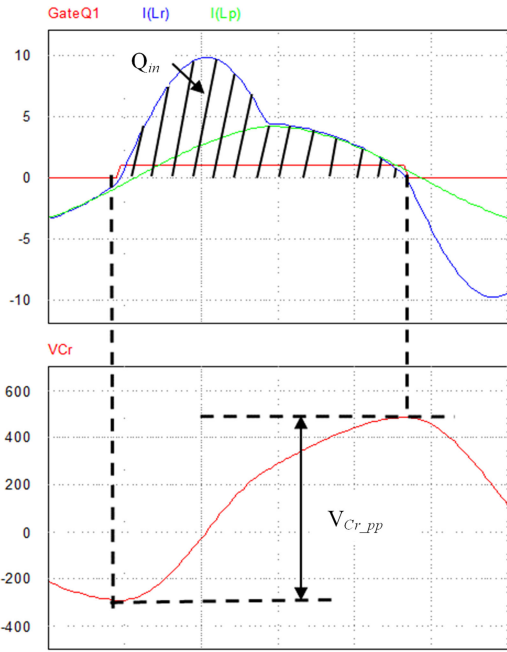


Fig. 12. C_r charging waveform at minimum frequency.

entire input voltage range 250–400 V. For aggressive designs, the f_{\min} could be chosen at the ZVS and ZCS boundary, where the resonant tank critically achieves the peak voltage gain (1.6 in this case). In this scenario, the resonant tank will have the maximum current stress, and the series capacitor C_r will have the maximum voltage stress. In practical designs, a reasonable margin should be considered for the input voltage, so that the entire range will have ZVS operation.

The selection of the minimum switching frequency f_{\min} should follow a similar strategy as the selection of the resonant frequency f_r , especially the magnetic component design and EMI design should be primarily considered. A widely acknowledged empirical value of f_{\min} is between 0.5 to 0.8 times f_r .

In this design example, 150 kHz as minimum switching frequency is selected as the starting point for 250 V input. The actual f_{\min} might have some deviation from this 150 kHz but can be compensated by one or two iterations. Voltage margin is not considered in this step, because FHA tends to underestimate the voltage gain, thus some margin is automatically left there.

C. C_r Selection Based on Voltage Stress at f_{\min}

For 250 V operation, at the selected of 150 kHz, the converter achieves peak voltage gain, and the resonant tank is pure resistive. Thus, the current on the primary side is critically in phase with the input square-wave voltage. That is to say, in half switching cycle, the resonant current will charge the resonant capacitor C_r from its minimum value to its maximum value [31]–[33]. The charging process is illustrated in Fig. 12.

Assuming 100% efficiency, the total charge Q_{in} in one switching cycle could be calculated by (5), in which $V_{\text{in},\min}$ is the minimum input voltage; P_o is the average output power; f_{\min} is the

minimum switching frequency

$$E_{\text{cycle}} = V_{\text{in},\min} Q_{\text{in}} = \frac{P_o}{f_{\min}}. \quad (5)$$

For a given capacitor value C_r , the voltage stress V_{Cr} can be calculated by (6), where $V_{Cr,\text{pk}}$ and $V_{Cr,\text{pp}}$ are the peak value and the peak-to-peak value of the capacitor voltage. It should be noted that this equation is true only at the peak gain point, where the resonant tank is pure resistive

$$V_{Cr,\text{pk}} = \frac{V_{Cr,\text{pp}}}{2} = \frac{Q_{\text{in}}}{2C_r}. \quad (6)$$

Combining (5) and (6), the minimum C_r value can be obtained in (7) with specifying the maximum voltage stress $V_{Cr,\text{pk}}$ on the capacitor C_r

$$C_{r,\min} = \frac{P_o}{2V_{Cr,\text{pk}} \cdot V_{\text{in},\min} \cdot f_{\min}}. \quad (7)$$

In this design, substitute in (7) with P_o as 500 W, $V_{\text{in},\min}$ as 250 V, f_{\min} of 150 kHz, and considering that the maximum ac peak voltage ratings ($V_{Cr,\text{pk}}$) for off-the-shelf film capacitors are around 350 V at 150 kHz [34], the minimum C_r value can be calculated as follows: $C_r = \frac{500\text{W}}{2*350\text{V}*250\text{V}*150*10^3\text{kHz}} = 19 \text{ nF}$.

In the case that the output power is low, the calculated minimum $C_{r,\min}$ value from (7) will be small. The C_r value designed by other methods is usually larger than the calculated minimum value. This automatically implies that the capacitor voltage stress is not a concern for low power applications. For high power applications, however, conventional design methods would suggest smaller C_r than the minimum value, despite the excessive voltage stress. In this case, the calculated minimum value should be accepted as C_r , because if a larger C_r value is used, the corresponding L_r and L_p will be smaller. This is generally opposed to the practice of reducing the resonant current.

D. L_r Selection Based on f_r at 400 V

Considering the resonant frequency determined in Step A, once the resonant capacitor is selected, the resonant inductor can be obtained in (8). In this design, f_r is 250 kHz, and C_r is 19 nF. Thus, the corresponding L_r is 21 μH

$$L_r = \frac{1}{(2\pi f_r)^2 C_r}. \quad (8)$$

E. C_p Selection Based on Voltage Stress at f_{\min}

Similar to C_r selection, the critical criterion for C_p selection is the voltage V_{Cp} . Generally speaking, a combination of small C_p and large L_p should be used to maximize 400 V efficiency.

As shown in the FHA model in Fig. 6, L_p and C_p can be equivalent to an inductor $L_{m,\text{eq}}$. The equivalent inductor $L_{m,\min}$ at 250 V input should be solved so as to get the current stress on C_p . Substituting into (2) with $G = nV_o/V_{\text{in}} = 1.6$, L_r of 21 μH , f_s of 150 kHz, f_r of 250 kHz, and also with $Q = \sqrt{L_r/C_r}/R_{\text{ac}}$, in which $R_{\text{ac}} = \frac{8n^2}{\pi^2} \cdot \frac{V_o^2}{P_o}$, $n = 17$, V_o of 12 V, and P_o of 500 W, the $L_{m,\min}$ can be solved. In this case, $L_{m,\min}$ is 57 μH .

It should be noted that the calculation error of $L_{m,\min}$ is the major source of error in this design routine. Due to the absence

of high-order harmonics, the predicted voltage gain at f_{\min} by the FHA method is lower than the actual gain. Then, to reach the same gain requirement, FHA will suggest lower $L_{m,\min}$, which will further impact the selection of C_p and L_p . A fine tune process will be introduced in a later part.

Based on the FHA model, the current in the parallel branch can be calculated in (9), in which $I_{p,\text{pk},f_{\min}}$ is the peak value of the parallel current at f_{\min} ; $L_{m,\min}$ is the equivalent magnetizing inductance at f_{\min}

$$I_{p,\text{pk},f_{\min}} = \frac{4}{\pi} n V_o \cdot \frac{1}{2\pi f_{\min} L_{m,\min}}. \quad (9)$$

The ac peak voltage stress for given C_p value can be calculated by (10), in which $V_{C_p,\text{pk},f_{\min}}$ is the peak value of the C_p voltage stress at f_{\min} ; X_{C_p} is the impedance of C_p at f_{\min}

$$V_{C_p,\text{pk},f_{\min}} = I_{p,\text{pk},f_{\min}} X_{C_p} = \frac{I_{p,\text{pk},f_{\min}}}{2\pi f_{\min} C_p}. \quad (10)$$

Then combining (9) and (10), the minimum C_p value is given in the following equation:

$$C_{p,\min} = \frac{n V_o}{\pi^3 f_{\min}^2 L_{m,\min} V_{C_p,\text{pk},f_{\min}}}. \quad (11)$$

In this design example, substitute into (11) with $n = 17$, V_o of 12 V, f_{\min} of 150 kHz, and 57 μ H as $L_{m,\min}$ and 350 V as peak voltage stress, the minimum C_p value is 14.6 nF.

F. L_p Selection Based on $L_{m,\min}$ at f_{\min}

For a given C_p , there is one and only one L_p that pairs with it, so that the equivalent $L_{m,\min}$ is as determined in Step E at the minimum frequency. The L_p value can be calculated by (1). With 57 μ H as $L_{m,\min}$, 150 kHz as f_{\min} , and 14.6 nF as C_p , in this example, L_p is 134 μ H.

G. Fine Tune of the Parameters With PSIM Simulation

As widely acknowledged, the accuracy of FHA degrades when the switching frequency is away from the resonant point. Specifically, in this case, a smaller-than-actual $L_{m,\min}$ value is predicted, which leads to a larger C_p and smaller L_p selection. The reverse correlation of $L_{m,\min}$ and C_p has been shown in (11). The error, however, can be easily corrected by simulation software, which has a much more accurate prediction of voltage gain.

The calculation of C_r and L_r results from the time domain equations and/or at resonant frequency, thus the accuracy is high. In this case, the C_r and L_r values from Steps C and D are used in PSIM to find the $L_{m,\min}$ value. If a margin for the minimum input voltage is intended, it should be performed in this stage. In this design example, $L_{m,\min}$ value of 85 μ H at $f_{\min} = 135$ kHz is found a reasonable setup, which provides a 20 V input voltage margin, so that actual $V_{in,\min}$ is 230 V. It should be noted that since the $V_{in,\min}$ and the f_{\min} are changed, the C_r value should also have a fine adjustment based on (7). In this case, C_r value is calibrated to 23 nF and L_r value is calibrated accordingly to 16 μ H.

TABLE I
PARAMETER DESIGN COMPARISON BETWEEN FHA AND SIMULATION
CALIBRATED RESULTS

	FHA Prediction	PSIM Calibration
L_r	21 μ H	17 μ H
C_r	19 nF	23 nF
L_p	134 μ H	216 μ H
C_p	14.6 nF	10.6 nF

TABLE II
PARAMETER DESIGN OF *LCLC* CONVERTER

L_r	16.5 μ H	L_p	230 μ H
C_r	23.5 nF	C_p	9.4 nF
f_r	250 kHz	f_{\min}	135 kHz

Then with the fine-tuned $L_{m,\min}$ value of 85 μ H, also substitute into (11) with $n = 17$, V_o of 12 V, f_{\min} of 135 kHz, and 400 V peak voltage stress at 135 kHz, the calibrated C_p value is 10.6 nF. The corresponding L_p is 216 μ H, which can be calculated by (1).

Table I shows the parameter design comparison between the FHA prediction and the PSIM calibrated results. As can be observed, the design of L_r and C_r values are rather true from the FHA, while the L_p and C_p have some deviation. Although FHA can provide a good predimensioning of the four resonant parameters, a calibration process is still considered necessary to provide a more realistic design result.

H. Practical Considerations of Capacitor Value

Besides the design considerations of the resonant frequency and minimum frequency selection as well as the minimum input voltage margin, the selection of capacitor values should also be practical. The 4.7 nF FKP-series film capacitor from WIMA appears to be a good balance of capacitance and voltage rating. In this design, total 23.5 nF consisting of five paralleled 4.7 nF capacitors are used as C_r , and total 9.4 nF consisting of two paralleled 4.7 nF capacitors are used as C_p . The final *LCLC* resonant tank design is shown in Table II.

IV. EXPERIMENT RESULTS

To verify the effectiveness of the *LCLC* topology and the design method, a prototype as shown in Fig. 13 is built to operate at 250–400 V input and 12 V/500 W rated load. Detailed design specification is shown in Table III. Due to the leakage inductance of the main transformer, the actual switching frequency is slightly lower than the designed one.

In the prototype, SRs are used to reduce the secondary rectifiers loss. Since *LCLC* converters have the same operation as that of the conventional *LLC* converter, a generic SR controller (IR11682S) for *LLC* converter is used. The controller will detect the conduction timing of the body diode and then turn ON the SR accordingly. Besides, an RCD delay circuit is used to offset the impact of the MOSFET package inductance, and help the controller capture the proper turn OFF timing [34].

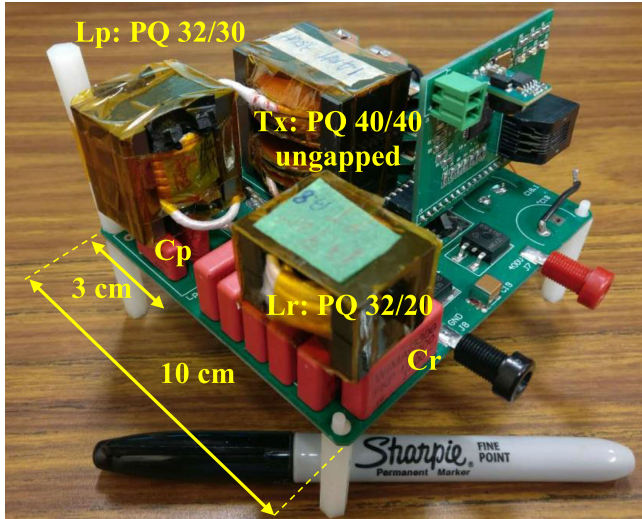


Fig. 13. Picture of the prototype.

TABLE III
DESIGN SPECIFICATION AND POWER TRAIN PARAMETERS OF LCLC
CONVERTER

V_{in}	250 V-400 V
V_o / I_o	12 V / 42 A
P_o	500 W
C_o	860 μ F (330 μ F E-cap *2 + 100 μ F ceramic *2)
T_x turns ratio	17:1
L_r	16.5 μ H
C_r	23.5 nF (4.7 nF * 5)
L_p	230 μ H
C_p	9.4 nF (4.7 nF * 2)
L_{lkg}	5 μ H
Designed 400V f_s	250 kHz
Designed 250V f_s	135 kHz

Fig. 14 shows the steady-state waveforms under 12 V/40 A full-load condition at 400 V input, at which the equivalent L_m is 180 μ H. As can be observed, the magnetizing current is ~ 1.5 A, which is a relatively small value. Thus, high efficiency at nominal 400 V can be achieved.

Fig. 15 shows the steady-state waveforms under 12 V/40 A full-load condition at 250 V input. At 250 V, the switching frequency reduces to 140 kHz, which has good agreement with the designed value. The magnetizing current peak value reaches 3.5 A, which implies the equivalent L_m is reduced to accommodate the low input voltage.

Fig. 16 shows the output voltage response to the input voltage drop under full load of 40 A. The output voltage can be maintained at 12 V even when the input voltage reduces to 220 V.

Fig. 17 shows the steady-state waveforms under 12 V/20 A half-load condition at 400 V input. Similar to the full-load case, the equivalent magnetizing inductor is around 180 μ H (even larger because switching frequency higher), and the magnetizing current is very small (1.5 A).

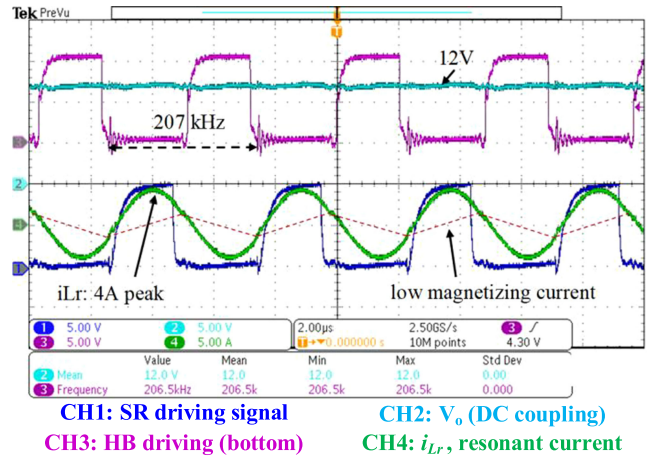


Fig. 14. 400 V input, 12 V/40 A output steady-state waveform.

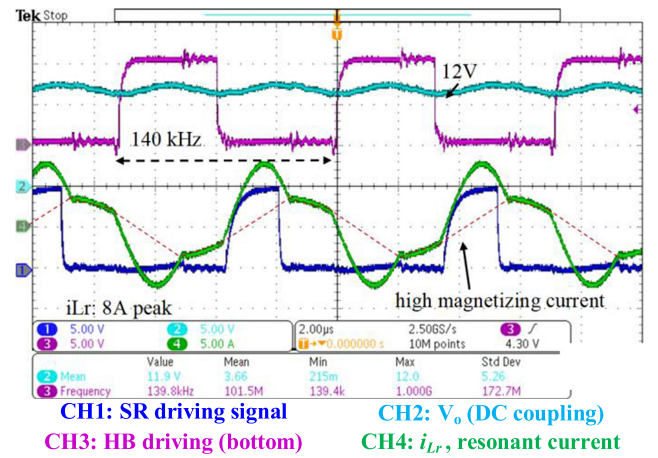


Fig. 15. 250 V input, 12 V/40 A output steady-state waveform.

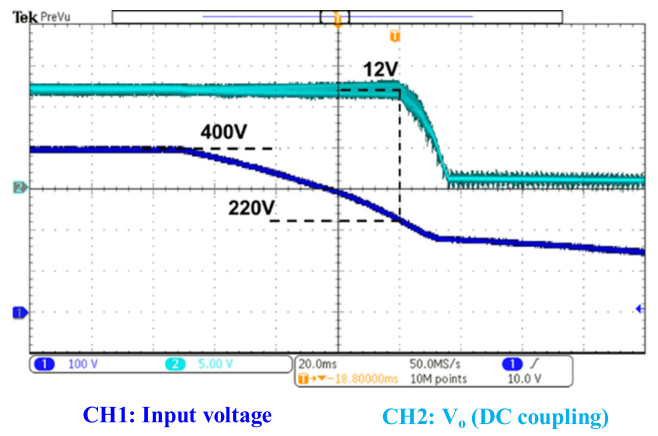


Fig. 16. Hold-up test under full load.

Fig. 18 shows the steady-state waveforms under 12 V/20 A full-load condition at 250 V input. The switching frequency reduces to 140 kHz, and the equivalent L_m is 70 μ H, so that the magnetizing current increase to 3.5 A.

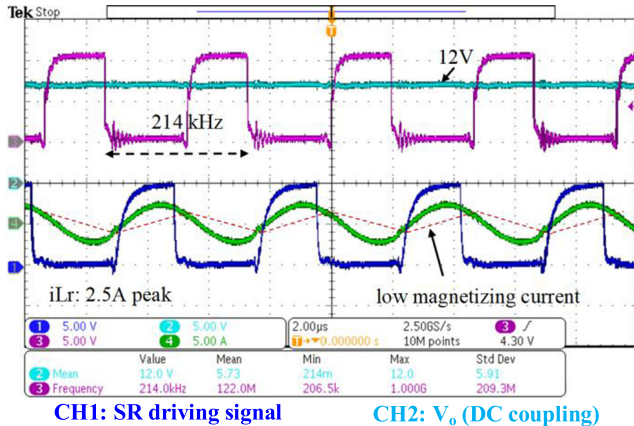


Fig. 17. 400 V input, 12 V/20 A output steady-state waveform.

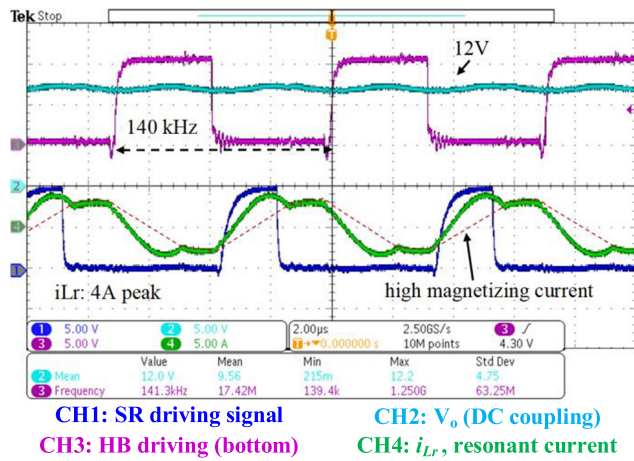


Fig. 18. 250 V input, 12 V/20 A output steady-state waveform.

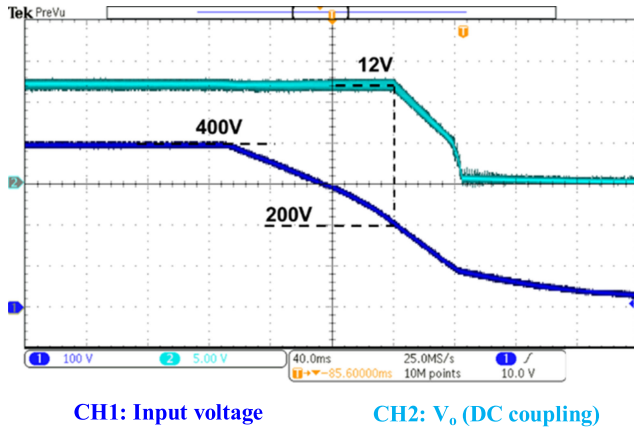


Fig. 19. Hold-up test under half load.

Fig. 19 shows the output voltage response to the input voltage drop under half load. The output voltage does not lose regulation until the input voltage reduces to 200 V.

Fig. 20 shows the efficiency comparison between the *LCLC* converter and a conventional *LLC* converter with same input voltage range from 250 to 400 V. The *LLC* converter magne-

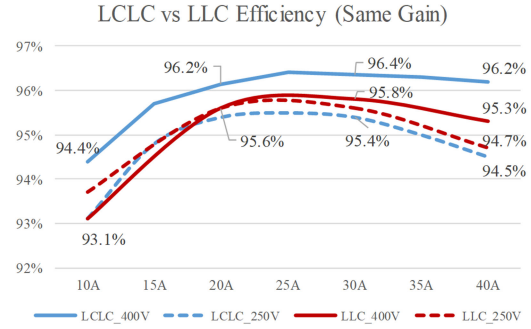
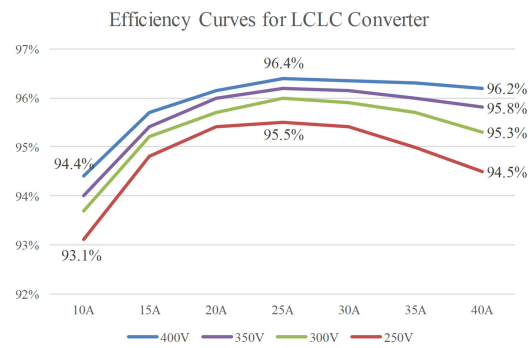
Fig. 20. Efficiency comparison of *LCLC* and *LLC* for 250 and 400 V.

Fig. 21. Efficiency curves of different input voltage level versus load.

tizing inductor is designed as $70 \mu\text{H}$, which is the same as the equivalent L_p value for *LCLC* converter at 250 V. As can be observed, at 400 V, the efficiency of *LCLC* (solid blue) is generally 1% higher than the conventional *LLC* (solid red), thanks to the larger equivalent L_p of $180 \mu\text{H}$. The front-end system is expected to benefit from this improvement, because the converter will operate for dominantly long time at 400 V. At 250 V, the *LCLC* converter efficiency (dashed blue) marginally trails the *LLC* converter (dashed red) by 0.2%, generally due to the additional loss on C_p . If the converter is designed for operating over a wide input range with equal chance at different input voltages, the *LCLC* converter can still benefit from the higher average efficiency over the conventional *LLC* converter.

Fig. 21 shows the measured efficiency at different input voltages: 250, 300, 350, and 400 V. The highest efficiency achieved is 96.4% at 400 V input, 60% load. For 400 V input full load, the achieved efficiency is 96.2%. As the input voltage reduces, the equivalent L_m is reduced, and the conduction loss increases, the efficiency is thus slightly degraded. For 250 V condition, the highest efficiency is 95.5% at 60% load. For full load, the measured efficiency is 94.3%.

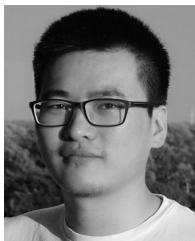
V. CONCLUSION

In this paper, *LCLC* resonant topology is examined and explained from the voltage gain improvement point of view. The *LCLC* topology achieves high efficiency for 400 V input as well as high voltage gain to satisfy the hold-up requirement. Besides, the *LCLC* converter enjoys high reliability, simple control, and low cost, because no active component is added, and generic

LCLC controller can be directly used. A design methodology focusing on the capacitor voltage stress is proposed to achieve optimal capacitor utilization in high power applications. A 250–400 V input, 500 W prototype has been built to verify the *LCLC* converter operation and the parameter design. The experiment results justify the feasibility and effectiveness of topology and the design method. With the *LCLC* converter prototype, the size increase is 10% as compared to the magnetics-integrated configuration, while there is no size increase when compared to core-separate configuration. A 1% of efficiency improvement is achieved for 400 V operation. This is believed a significant reduction of power consumption and carbon emissions for large facilities such as data centers.

REFERENCES

- [1] “Supercomputer top500,” 2014. [Online]. Available: <http://www.top500.org/featured/top-systems/>
- [2] J. Koomey, “Growth in data center electricity use 2005 to 2010,” Analytical Press, vol. 9, pp. 1–24, 2011.
- [3] B. Yang, “Topology investigation for front end DC/DC power conversion for distributed power system,” Ph.D. thesis, Virginia Polytechnic Institute and State University, Blacksburg, VA, USA, 2003.
- [4] D. Fu, B. Lu, and F. C. Lee, “1MHz high efficiency LLC resonant converters with synchronous rectifier,” in *Proc. IEEE Annu. Power Electron. Spec. Conf.*, 2007, pp. 2404–2410.
- [5] B. Yang, F. C. Lee, A. J. Zhang, and G. Huang, “LLC resonant converter for front end DC/DC conversion,” in *Proc. 17th Annu. IEEE Appl. Power Electron. Conf. Expo.*, 2002, vol. 2, pp. 1108–1112.
- [6] R. P. Severns, “Topologies for three-element resonant converters,” *IEEE Trans. Power Electron.*, vol. 7, no. 1, pp. 89–98, Jan. 1992.
- [7] D. Fu, F. C. Lee, and S. Wang, “Investigation on transformer design of high frequency high efficiency dc-dc converters,” in *Proc. 25th Annu. IEEE Appl. Power Electron. Conf. Expo.*, 2010, pp. 940–947.
- [8] S. De Simone, C. Adragna, C. Spini, and G. Gattavari, “Design-oriented steady-state analysis of LLC resonant converters based on FHA,” in *Proc. Int. Symp. Power Electron., Elect. Drives, Autom. Motion on*, 2006, pp. 200–207.
- [9] X. Fang *et al.*, “Efficiency-oriented optimal design of the LLC resonant converter based on peak gain placement,” *IEEE Trans. Power Electron.*, vol. 28, no. 5, pp. 2285–2296, May 2013.
- [10] H. Wang, Y. Chen, Y.-F. Liu, J. Afsharian, and Z. Yang, “A new LLC converter family with synchronous rectifier to increase voltage gain for hold-up application,” in *Proc. IEEE Energy Convers. Congr. Expo.*, 2015, pp. 5447–5453.
- [11] D. Wang and Y. F. Liu, “A zero-crossing noise filter for driving synchronous rectifiers of LLC resonant converter,” *IEEE Trans. Power Electron.*, vol. 29, no. 4, pp. 1953–1965, Apr. 2014.
- [12] W. Feng, P. Mattavelli, F. C. Lee, and D. Fu, “LLC converters with automatic resonant frequency tracking based on synchronous rectifier (SR) gate driving signals,” in *Proc. 26th Annu. IEEE Appl. Power Electron. Conf. Expo.*, 2011, pp. 1–5.
- [13] Y. Xing, L. Huang, X. Cai, and S. Sun, “A Combined Front End DC / DC Converter,” in *Proc. 18th Annu. IEEE Appl. Power Electron. Conf. Expo.*, 2003, vol. 2, pp. 1095–1099.
- [14] B. Yang, P. Xu, and F. C. Lee, “Range winding for wide input range front end DC/DC converter,” in *Proc. 6th Annu. IEEE Appl. Power Electron. Conf. Expo.*, 2001, vol. 1, pp. 476–479.
- [15] M. Y. Kim, B. C. Kim, K. B. Park, and G. W. Moon, “LLC series resonant converter with auxiliary hold-up time compensation circuit,” in *Proc. 8th Int. Conf. Power Electron.*, 2011, pp. 628–633.
- [16] B. C. Kim, K. B. Park, G. W. Moon, and T. S. Jeju, “LLC Resonant Converter with asymmetric PWM for hold up time,” in *Proc. 8th Int. Conf. Power Electron.*, 2011, pp. 38–43.
- [17] B.-C. Kim, K.-B. Park, S.-W. Choi, and G.-W. Moon, “LLC series resonant converter with auxiliary circuit for hold-up time,” in *Proc. 31st Int. Telecommun. Energy Conf.*, Oct. 2009, pp. 1–4.
- [18] I. H. Cho, Y. Do Kim, and G. W. Moon, “A half-bridge LLC resonant converter adopting boost PWM control scheme for hold-up state operation,” *IEEE Trans. Power Electron.*, vol. 29, no. 2, pp. 841–850, Feb. 2014.
- [19] J. W. Kim and G. W. Moon, “A New LLC series resonant converter with a narrow switching frequency variation and reduced conduction losses,” *IEEE Trans. Power Electron.*, vol. 29, no. 8, pp. 4278–4287, Aug. 2014.
- [20] H. Wu, T. Mu, X. Gao, and Y. Xing, “A secondary-side phase-shift-controlled LLC resonant converter with reduced conduction loss at normal operation for hold-up time compensation application,” *IEEE Trans. Power Electron.*, vol. 30, no. 10, pp. 5352–5357, Oct. 2015.
- [21] H. Wang, Y. Chen, P. Fang, Y. F. Liu, J. Afsharian, and Z. Yang, “An LLC converter family with auxiliary switch for hold up mode operation,” *IEEE Trans. Power Electron.*, vol. 32, no. 6, pp. 4291–4306, Jun. 2017.
- [22] Y. Chen, H. Wang, Y. F. Liu, J. Afsharian, and Z. Yang, “LLC converter with auxiliary switch for hold up mode operation,” in *Proc. IEEE Appl. Power Electron. Conf. Expo.*, 2016, pp. 2312–2319.
- [23] Y. Chen, H. Wang, Z. Hu, Y.-F. Liu, J. Afsharian, and Z. Yang, “LCLC resonant converter for hold up mode operation,” in *Proc. IEEE Energy Convers. Congr. Expo.*, 2015, pp. 556–562.
- [24] R. Beiranvand, S. Member, B. Rashidian, and M. R. Zolghadri, “Optimizing the normalized dead-time and maximum switching frequency of a wide-adjustable-range LLC resonant converter,” *IEEE Trans. Power Electron.*, vol. 26, no. 2, pp. 462–472, Feb. 2011.
- [25] R. Beiranvand, B. Rashidian, M. R. Zolghadri, and S. M. Hossein Alavi, “A design procedure for optimizing the LLC resonant converter as a wide output range voltage source,” *IEEE Trans. Power Electron.*, vol. 27, no. 8, pp. 3749–3763, Aug. 2012.
- [26] H. Figge, T. Grote, N. Frohleke, J. Bocker, and F. Schafmeister, “Overcurrent protection for the LLC resonant converter with improved hold-up time,” in *Proc. 26th Annu. IEEE Appl. Power Electron. Conf. Expo.*, 2011, pp. 13–20.
- [27] T. Liu, Z. Zhou, A. Xiong, J. Zeng, and J. Ying, “A novel precise design method for LLC series resonant converter,” in *Proc. 28th Annu. Int. Telecommun. Energy Conf.*, 2006, pp. 1–6.
- [28] B. Lu, W. Liu, Y. Liang, F. C. Lee, and J. D. Van Wyk, “Optimal design methodology for LLC resonant converter,” in *Proc. 21st Annu. IEEE Appl. Power Electron. Conf. Expo.*, 2006, pp. 533–538.
- [29] F. Musavi, M. Craciun, D. S. Gautam, and W. Eberle, “Control strategies for wide output voltage range LLC resonant DC/DC converters in battery chargers,” *IEEE Trans. Veh. Technol.*, vol. 63, no. 3, pp. 1117–1125, Mar. 2014.
- [30] R. Yu, G. K. Y. Ho, B. M. H. Pong, B. W.-K. Ling, and J. Lam, “Computer-aided design and optimization of high-efficiency LLC series resonant converter,” *IEEE Trans. Power Electron.*, vol. 27, no. 7, pp. 3243–3256, Jul. 2012.
- [31] Z. Hu, Y.-F. Liu, and P. C. Sen, “Cycle-by-cycle average input current sensing method for LLC resonant topologies,” in *Proc. IEEE Energy Convers. Congr. Expo.*, 2013, pp. 167–174.
- [32] Z. Hu, L. Wang, H. Wang, Y. F. Liu, and P. C. Sen, “An accurate design algorithm for LLC resonant converters part I,” *IEEE Trans. Power Electron.*, vol. 31, no. 8, pp. 5435–5447, Aug. 2016.
- [33] Z. Hu, L. Wang, Y. Qiu, Y. F. Liu, and P. C. Sen, “An accurate design algorithm for LLC resonant converters part II,” *IEEE Trans. Power Electron.*, vol. 31, no. 8, pp. 5448–5460, Aug. 2016.
- [34] WIMA, “WIMA FKP 1 datasheet,” 2018. [Online]. Available: <https://www.wima.de/en/our-product-range/pulse-capacitors/fkp-1/>. Accessed on: Jul. 4, 2018.
- [35] D. Wang and Y. F. Liu, “A zero-crossing noise filter for driving synchronous rectifiers of LLC resonant converter,” *IEEE Trans. Power Electron.*, vol. 29, no. 4, pp. 1953–1965, Apr. 2014.



Yang Chen (S’14–M’17) received the B.Sc. and M.Sc. degrees in electrical engineering from the Beijing Institute of Technology, Beijing, China, in 2011 and 2013, respectively, and the Ph.D. degree in electrical and computer engineering from Queen’s University, Kingston, ON, Canada, in 2017.

His research interests include topology and control of power converters for datacenter and server power supplies, miniaturized resonant converters with wide voltage range for notebook and cellphone fast charging, and high-performance dc–dc converters and ac–dc chargers for EV. He has authored 20 technical papers published in IEEE journals and conferences and has 6 US/PCT patents pending.



Hongliang Wang (M'12–SM'15) received the B.Sc. degree in electrical engineering from the Anhui University of Science and Technology, Huainan, China, in 2004, and the Ph.D. degree in electrical engineering from the Huazhong University of Science and Technology, Wuhan, China, in 2011.

From 2004 to 2005, he worked as an Electrical Engineer with Zhejiang Hengdian Thermal Power Plant. From 2011 to 2013, he worked as a Senior System Engineer with Sungrow Power Supply Co., Ltd. From 2013 to 2018, he worked as a Postdoctoral Fellow with Queen's University. Since 2018, he has been with Hunan University, Changsha, China, where he is currently a Professor with the College of Electrical and Information Engineering. His current research interests include multilevel topology, high-gain topology, parallel technology, and virtual synchronous generator (VSG) technology for photovoltaic application and microgrids application; resonant converters and server power supplies; and LED drivers. He has authored more than 60 technical papers in journals and conferences. He is the inventor/co-inventor of 41 China issued patents, 2 U.S. issued patents, 11 U.S. patents pending, and 9 PCT patents pending.

Dr. Wang is currently a Senior Member of China Electro-Technical Society (CES) and a Senior Member of China Power Supply Society (CPSS). He serves as a member of CPSS Technical Committee on Standardization, a member of CPSS Technical Committee on Renewable Energy Power Conversion, a China Expert Group Member of IEC Standard TC8/PT 62786, a Vice-Chair of IEEE Kingston Section, a Session Chair of ECCE 2015 and ECCE2017, and a TPC Member of ICEMS2012.



Zhiyuan Hu (S'10–M'15) received the Ph.D. degree in electrical and computer engineering from Queen's University, Kingston, ON, Canada, in 2014.

From 2007 to 2010, he was with Potentia Semiconductor Corp. and Power Integrations Inc. From 2014 to 2018, he was with Texas Instruments Inc. He is currently with Apple Inc., Cupertino, CA, USA. He has one U.S. patent and several innovations. His research interests include dc–dc converters and digital control.



Yan-Fei Liu (M'94–SM'97–F'13) received the bachelor's and master's degree from Zhejiang University, Hangzhou, China, in 1984 and 1987, respectively, and the Ph.D. degree from Queen's University, Kingston, ON, Canada, in 1994.

He was a Technical Advisor with the Advanced Power System Division, Nortel Networks, Ottawa, ON, Canada, from 1994 to 1999. Since 1999, he has been with Queen's University, where he is currently a Professor with the Department of Electrical and Computer Engineering. His current research interests include digital control technologies for high efficiency, fast dynamic response dc–dc switching converter and ac–dc converter with power factor correction, resonant converters and server power supplies, and LED drivers. He has authored more than 230 technical papers in the IEEE Transactions and conferences and holds 25 U.S. patents.

Dr. Liu is also a Principal Contributor for two IEEE standards. He is a Fellow of Canadian Academy of Engineering and received Modeling and Control Achievement Awards from IEEE Power Electronics Society. He was the recipient of the Premier's Research Excellence Award in 2000 in Ontario, Canada, and also the Award of Excellence in Technology in Nortel in 1997. He is currently the Vice President of Technical Operations of IEEE Power Electronics Society (PELS, from 2017 to 2018). He has been an Editor of IEEE JOURNAL OF EMERGING AND SELECTED TOPICS OF POWER ELECTRONICS (IEEE JESTPE) since 2013. He will be the General Chair of ECCE 2019 to be held in Baltimore, MD, USA, in 2019. His major service to IEEE is listed below: a Guest Editor-in-Chief for the special issue of Power Supply on Chip of IEEE TRANSACTIONS ON POWER ELECTRONICS from 2011 to 2013; a Guest Editor for special issues of JESTPE: Miniaturization of Power Electronics Systems in 2014 and Green Power Supplies in 2016; as Co-General Chair of ECCE 2015 held in Montreal, QB, Canada, in September 2015; the Chair of PELS Technical Committee (TC1) on Control and Modeling Core Technologies from 2013 to 2016; and the Chair of PELS Technical Committee (TC2) on Power Conversion Systems and Components from 2009 to 2012.



Xiaodong Liu was born in Jilin, China, in 1971. He received the B.Sc. and M.Sc. degrees in electrical engineering from Liaoning Technical University, Fuxin, China, in 1993 and 1996, respectively, and the Ph.D. degree from Zhejiang University, Hangzhou, China, in 1999.

From July 1999 to July 2003, he worked as an Engineer with Xuji-Hitachi Corporation, where he was responsible for the design and specification of 500kv busbar relay. Since August 2003, he joined the Anhui University of Technology, Maanshan, China, where he is currently a Professor with the Department of Electrical and Information Engineering. His research interests include topologies and modeling of switching converters, digital control techniques for dc–dc converters, and arbitrary waveform power amplifier based on SLH, motor design and driving control. He has authored and coauthored more than 40 technical papers in the IEEE Transactions and conferences.



Jahangir Afsharian received the B.S. and M.S. degrees in electrical engineering from Ryerson University, Toronto, ON, Canada, in 2006 and 2009, respectively. He is currently working toward the Ph.D. degree at Ryerson University.

From 2009 to 2011, he was a Research and Development (R&D) Engineer with the Communications and Power Industries, Georgetown, ON, Canada, where he was involved on the design of resonant converter LCC and high-voltage transformer for X-ray medical equipment. From end of 2011 to present, he is a Senior Electrical Engineer with the Advanced Development Group, Murata Power solution, Toronto, where he is involved in the power electronics ac–dc power-factor-correction and dc–dc converter. His current research interests include three-phase matrix-based rectifier for battery charger and data center applications.



Zhihua (Alex) Yang was born in Hubei, China. He received the B.S. degree from the Hubei Institute of Technology, Hubei, in 1993, and the M.S. degree from Queen's University, Kingston, ON, Canada, in 2005, both in electrical engineering.

He worked as a Design Engineer with Wuhan Zhouji Telecom Power Supply Corporation from 1993 to 2002. He has been a Design Engineer with the Advanced Research Center, Paradigm Electronics, Inc., Canada, during 2005–2007. He joined Murata Power Solutions Inc., Markham, ON, Canada, in 2007. Since 2007, he has been working as a Design Engineer, a Senior Design Engineer, and a Principal Design Engineer. He is currently holding the position of the Director of Product Development with Murata Power Solutions, Inc. His research interests include high switching frequency, high power density, and high-efficiency switching mode power suppliers.